

DOI:10.16781/j.0258-879x.2017.09.1165

超高分辨率 CT 靶扫描对肺结节的诊断价值

朱慧媛^{1,2}, 张 莲^{1,3}, 王亚丽², 杨 洋², 毛海霞², 李 飞², 孙希文^{2*}

1. 同济大学医学院影像医学与核医学系, 上海 200092

2. 同济大学附属上海市肺科医院影像科, 上海 200433

3. 嘉定区中医医院影像科, 上海 201800

[摘要] **目的** 探讨 1 024 超高分辨率 CT 靶扫描对直径 8 mm 以下肺结节的诊断价值及其对随访方案的影响。

方法 前瞻性分析 2015 年 7 月—2016 年 8 月于同济大学附属上海市肺科医院影像科门诊进行 1 024 超高分辨率 CT 靶扫描的 57 例患者的 67 个肺结节资料。肺结节平均直径为 (5.97 ± 1.34) mm。对其中 32 个结节进行手术切除, 病理结果提示 2 个结节为良性, 9 个结节为不典型腺瘤样增生(AAH), 14 个结节为原位腺癌(AIS), 7 个结节为微浸润腺癌(MIA); 16 个结节怀疑恶性但未手术; 19 个结节随访或考虑良性病灶。对 67 个肺结节均行常规 CT 扫描和 1 024 超高分辨率 CT 靶扫描, 由 3 位有 3~10 年工作经验的影像科医师阅片, 评价图像质量、判断结节类型、评估诊断信心、给出诊断结果和处理方案, 并对阅片结果进行统计学分析。**结果** 1 024 超高分辨率 CT 靶扫描在显示肺结节内部混杂密度、结节边缘、分叶征等方面优于常规 CT 检查 ($P < 0.05$), 两种扫描图像对判断纯磨玻璃结节和混杂密度结节的差异有统计学意义 ($P < 0.05$)。与常规 CT 比较, 1 024 超高分辨率 CT 靶扫描的诊断正确率增高 ($P < 0.01$), 医师诊断信心提高 ($P < 0.05$), 且基于两套图像给出的处理方案差异有统计学意义 ($P < 0.05$), 其差异主要体现为随访例数减少、手术例数和无需随访例数增加。**结论** 1 024 超高分辨率 CT 靶扫描对直径 8 mm 以下肺结节可较常规 CT 检查提供更好的图像质量。对通过常规 CT 检查难以确诊或诊断信心不充足的结节, 可采用 1 024 超高分辨率 CT 靶扫描进一步检查。

[关键词] 肺结节; 靶扫描; 超高分辨率; X 线计算机体层摄影术

[中图分类号] R 563 **[文献标志码]** A **[文章编号]** 0258-879X(2017)09-1165-06

Diagnosis value of targeted ultra high-resolution CT scanning for pulmonary nodules

ZHU Hui-yuan^{1,2}, ZHANG Lian^{1,3}, WANG Ya-li², YANG Yang², MAO Hai-xia², LI Fei², SUN Xi-wen^{2*}

1. Imaging and Nuclear Medicine, Tongji University School of Medicine, Shanghai 200092, China

2. Department of Radiology, Shanghai Pulmonary Hospital, Tongji University, Shanghai 200433, China

3. Department of Radiology, Jiading Hospital of Traditional Chinese Medicine, Shanghai 201800, China

[Abstract] **Objective** To evaluate the diagnostic value of targeted 1 024 ultra high-resolution CT scanning for the pulmonary nodules under 8 mm in diameter and its effect on follow-up protocols. **Methods** A total of 67 pulmonary nodules with a mean diameter of (5.97 ± 1.34) mm in 57 patients undergoing targeted scans at Department of Radiology, Shanghai Pulmonary Hospital, Tongji University between July 2015 and August 2016 were analyzed prospectively. Two of 32 nodules with surgical resection were benign, 9 were atypical adenomatous hyperplasia (AAH), 14 were adenocarcinoma *in situ* (AIS), and 7 were minimally invasive adenocarcinoma (MIA). Sixteen nodules were considered to be malignant but not resected and 19 nodules were considered as benign lesions or required follow-up. The 67 pulmonary nodules were examined by conventional CT scan and targeted 1 024 ultra high-resolution CT scan. Three radiologists with 3-10 years of experience in imaging evaluated the image quality, type of nodules, diagnostic confidence using a 5-point score and gave the diagnosis result and treatment method. The film-reading results were analyzed using SPSS software. **Results** The images obtained by the targeted 1 024 ultra high-resolution CT scan were significantly superior to that of conventional CT in showing the margin of nodules, internal component, lobulation sign and other aspects ($P < 0.05$). There were significant differences in judging the pure ground-glass opacity (GGO) nodules and mixed

[收稿日期] 2017-02-26 **[接受日期]** 2017-04-22

[基金项目] 上海市市级医院临床辅助科室能力建设项目(SHDC22015037)。Supported by Project of Capacity Construction of Clinical Assisting Departments of Shanghai Municipal Hospitals (SHDC22015037)。

[作者简介] 朱慧媛, 硕士生, 住院医师。E-mail: june212300@126.com

* 通信作者 (Corresponding author)。Tel: 021-65115006-3082, E-mail: sunxiwen93938@126.com

GGO nodules between the two kinds of CT images ($P < 0.05$). The diagnostic accuracy of targeted 1 024 ultra high-resolution CT scan was significantly increased versus the conventional CT scan ($P < 0.05$), and the same was true for the diagnostic confidence ($P < 0.05$). The treatment methods given by the two kinds of CT images were significantly different ($P < 0.05$), which was reflected by the decreasing number of follow-up cases and increasing numbers of surgical cases and no follow-up cases. **Conclusion** The targeted 1 024 ultra high-resolution CT scan can provide a better image quality for pulmonary nodules below 8 mm in diameter. For patients with pulmonary nodules which are difficult to diagnose or with insufficient confidence, further examination should be performed using a targeted 1 024 ultra high-resolution scan.

[Key words] pulmonary nodules; targeted scanning; ultra high-resolution; X-ray computed tomography

[Acad J Sec Mil Med Univ, 2017, 38(9): 1165-1170]

随着高分辨率 CT (high-resolution CT, HRCT) 技术的发展以及低剂量 CT 在肺癌筛查中的广泛应用, 肺结节的筛查与诊断取得一定成果^[1-4]。然而结节的性质逐渐成为人们关注的焦点。常规 HRCT 采用 512×512 矩阵, 其空间分辨率仅有 $0.23 \sim 0.35$ mm, 对判断 1 cm 以上肺结节的良恶性改变较为敏感, 而对 1 cm 以下结节的诊断结果并不可靠。近年来, $1\ 024 \times 1\ 024$ 超高分辨率 CT (以下简称 1 024 超高分辨率 CT) 的发展进一步提高了图像质量。“靶扫描”这一概念最早由李惠民等^[5]提出, 该技术利用缩小扫描视野 (field of view, FOV) 提高图像分辨率, 有助于显示肺部小结节更多的影像学特征。本研究采用 1 024 超高分辨率 CT 对直径 8 mm 以下肺结节进行靶扫描, 分析该方法的诊断价值。

1 资料和方法

1.1 研究设计 本研究采用前瞻性研究方法, 研究

对象为 2015 年 7 月—2016 年 8 月于同济大学附属上海市肺科医院影像科门诊进行 1 024 超高分辨率 CT 靶扫描的患者。本研究获得同济大学附属上海市肺科医院伦理委员会批准, 患者自愿接受检查并签署知情同意书。患者均经体格检查发现肺部结节, 既往健康。对患者进行常规 CT 扫描及 1 024 超高分辨率 CT 靶扫描, 随后经 3 位有 3~10 年工作经验的影像科医师阅片, 对两套 CT 扫描图像中肺结节内部混杂密度、结节边缘、分叶征、胸膜凹陷征 4 个方面的显示质量进行评分: 1~5 分表示图像质量逐级提高, 1 分表示图像质量很差, 无法辨认; 5 分表示图像质量很好, 征象及边缘显示非常清楚 (图 1)。图 1 仅从结节内部混杂密度角度进行评分说明, 而非对整体图像质量的评分。评分后对肺结节是否为纯磨玻璃结节进行判断, 并给出诊断和处理建议。诊断信心采用 5 级评分, 1~5 级表示信心逐级增加, 1 级表示缺乏信心, 5 级表示信心充分。

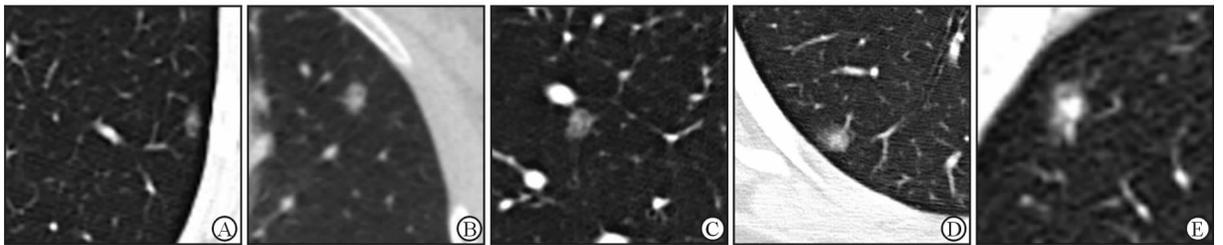


图 1 从肺结节内部混杂密度角度进行图像质量评分的图示说明

Fig 1 Illustration of score-assigning from aspect of internal density of the pulmonary nodules

A: Scored “1”, indicating the internal mixed density component was unidentified; B: Scored “2”, indicating the internal mixed density component was visible but not obvious or blurry; C: Scored “3”, indicating the internal mixed density component was visible and obvious; D: Scored “4”, indicating the internal mixed density component was very obvious and the margin was well defined; E: Scored “5”, indicating the internal mixed density component was extremely obvious and the margin was extremely clear

1.2 患者信息 纳入研究 57 例患者 67 个结节, 其中男性患者 21 例, 女性 36 例, 年龄 28~66 岁, 平均年龄 (45.2 ± 10.5) 岁。靶扫描的 67 个结节的平均直径为 (5.97 ± 1.34) mm, 最大为 7.81 mm, 最小为

2.60 mm。对 32 个结节进行手术, 病理结果显示其中 2 个为良性结节、9 个为不典型腺瘤样增生 (atypical adenomatous hyperplasia, AAH)、14 个为原位腺癌 (adenocarcinoma *in situ*, AIS)、7 个为

微浸润腺癌 (minimally invasive adenocarcinoma, MIA); 16个结节怀疑恶性但未手术, 19个结节建议随访或考虑良性病灶。

1.3 扫描参数和流程 本研究采用荷兰 PHILIPS-Brilliance 128 排螺旋 CT 进行扫描。患者取仰卧位, 双臂高举过头, 扫描过程中均屏气, 无增强。扫描参数见表 1, 扫描完成后的 CT 图像数据传输至 Extended Brilliance™ Workplace V3.5 进行阅片和 多平面重建。

表 1 常规 CT 和 1 024 超高分辨率 CT 靶扫描的扫描参数

Tab 1 Scan parameters of conventional CT and targeted 1 024 ultra high-resolution CT

Parameter	Conventional CT	Targeted CT
Tube voltage U/kV	120	120
Tube current I/mA	100	200
Beam collimation (mm×mm)	0.62×128	0.62×54
DLP (mGy·cm)	280.3	191.3
sFOV d/mm	350	100
Rotation time t/s	0.5	0.5
Helical pitch d/mm	0.804	0.578
Matrix	512×512	1 024×1 024
Slice d/mm	1.0	1.0
Window width (HU)	1 200	1 200
Window center (HU)	-450	-450

Targeted CT: Targeted 1 024 ultra high-resolution CT. DLP: Dose-length product; sFOV: Scan field of view; HU: Hounsfield unit

表 2 常规 CT 与 1 024 超高分辨率 CT 靶扫描的诊断正确率

Tab 2 Diagnostic accuracy of conventional CT and targeted 1 024 ultra high-resolution CT scans

Pathology	N	Right diagnosis based on conventional CT	Right diagnosis based on targeted 1 024 ultra high-resolution CT	$n(\%)$	P value
Benign	2	0(0.00)	1(50.00)		
AAH	9	2(22.22)	4(44.44)		0.167
AIS	14	11(78.57)	12(85.71)		0.396
MIA	7	4(57.14)	6(85.71)		1.000
Total	32	17(53.13)	23(71.88)		<0.001

AAH: Atypical adenomatous hyperplasia; AIS: Adenocarcinoma *in situ*; MIA: Minimally invasive adenocarcinoma

2.3 图像评分结果 两种 CT 扫描方式的阅片结果详见表 3。结果显示, 1 024 超高分辨率 CT 靶扫描图像对结节边缘、内部混杂密度、分叶征的显示较常规 CT 更为清晰, 评分高于常规 CT ($P<0.05$)。但对胸膜凹陷征的显示与常规 CT 相比差异无统计学意义 ($P>0.05$)。18 个常规 CT 图像显示为纯磨玻璃或不能确定的结节经 1 024 超高分辨率 CT 靶

1.4 统计学处理 应用 SPSS 17.0 软件进行数据分析。计量资料以 $\bar{x}\pm s$ 表示, 计数资料以百分比表示; 其中组间纯磨玻璃结节的判断、诊断结果及处理建议等分类变量的比较采用 McNemar 检验, 诊断正确率采用 Fisher 确切概率检验, 影像学征象以及诊断信心采用 Wilcoxon 秩和检验。检验水准 (α) 为 0.05。评分一致性检验采用 Kappa (κ) 值检验: 0.00~0.20 表示一致性很差, 0.21~0.40 一般, 0.41~0.60 中等, 0.61~0.80 良好, 0.81~1.00 非常好。

2 结果

2.1 医师诊断一致性检验 由 3 位阅片医师对 8 项阅片项目进行评价, 共进行 48 次一致性检验。 κ 值最大为 0.79, 最小为 -0.02, 中位数为 0.51, 医师诊断一致性为中等。

2.2 诊断正确率 将依据两套图像得出的诊断结果分别与病理结果进行比较 (当 3 位阅片医师诊断结果不一致时, 须经协商给出统一结果), 结果见表 2。1 024 超高分辨率 CT 靶扫描的诊断正确率为 71.88%, 较常规 CT (53.13%) 增高, 且差异具有统计学意义 ($P<0.001$)。

扫描检查后被判定为混杂磨玻璃结节 ($P<0.05$)。基于两种扫描图像给出的诊断结果及处理方案差异均有统计学意义 ($P<0.05$), 其中处理方案差异主要体现在手术例数和无需随访例数增加, 随访例数减少。此外, 医师采用 1 024 超高分辨率 CT 靶扫描的诊断信心高于常规 CT ($P<0.05$)。

表3 两种CT扫描图像的阅片结果

Tab 3 Reading results of two kinds of CT imaging

N=67

	Conventional CT	Targeted 1 024 ultra high-resolution CT	P value
Interface $\bar{x}\pm s$	3.18±0.40	3.89±0.46	<0.001
Density heterogeneity $\bar{x}\pm s$	2.83±0.51	3.33±0.57	<0.001
Lobulation sign $\bar{x}\pm s$	3.50±0.57	3.86±0.53	0.046
Pleural indentation $\bar{x}\pm s$	3.14±0.48	4.08±0.46	0.317
Classification of nodule <i>n</i> (%)			0.001
Pure GGO	29(43.28)	17(25.37)	
Mixed GGO	30(44.78)	48(71.64)	
Unidentified	8(11.94)	2(2.99)	
Diagnostic confidence $\bar{x}\pm s$	3.34±0.44	3.78±0.43	<0.001
Diagnosis <i>n</i> (%)			0.006
Benign	36(53.73)	28(41.79)	
Malignant	31(46.27)	39(58.21)	
Recommendation <i>n</i> (%)			0.009
No necessary for follow-up	10(14.93)	11(16.42)	
Follow-up	30(44.78)	17(25.37)	
Surgery	27(40.30)	39(58.21)	

GGO: Ground-glass opacity

2.4 典型病例图像 图2所示为4个结节的图像。由图2可见,1 024超高分辨率CT靶扫描图像中结节边缘更清晰,图像中叶间裂及血管边缘也更加清晰。相对于常规CT,1 024超高分辨率CT靶扫描

图像能显示出不同程度的密度不均以及内部高密度小颗粒,且混杂密度成分与周围磨玻璃成分边界更加清晰。

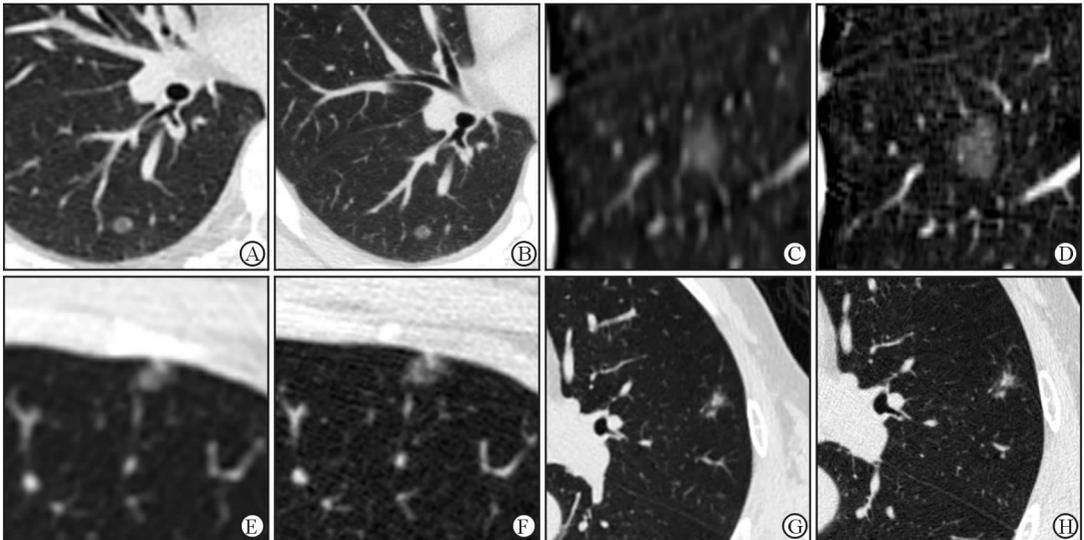


图2 4个肺结节的CT扫描图像

Fig 2 CT images of 4 representative pulmonary nodules

A, B: A 51-year-old female patient with atypical adenomatous hyperplasia (AAH). The nodule is located in the dorsal segment of the right lower lobe of the lung. The maximum diameter is 5.10 mm. C, D: A 31-year-old male patient with adenocarcinoma *in situ* (AIS). The nodule is located in the dorsal segment of the right lower lobe of the lung. The maximum diameter is 7.15 mm. E, F: A 29-year-old female patient with AIS. The nodule is located in the anterior segment of the left upper lobe of the lung. The maximum diameter is 5.50 mm. G, H: A 63-year-old male patient with minimally invasive adenocarcinoma (MIA). The nodule is located in the lingular segment of the left upper lobe of the lung. The maximum diameter is 6.90 mm. A, C, E, G: Cross-sectional image of conventional CT; B, D, F, H: Cross-sectional image of targeted 1 024 ultra high-resolution CT

3 讨论

AAH、AIS、MIA在HRCT影像上均可表现为纯磨玻璃结节,但其大小、密度、伴随征象等各有不同^[6]。在CT影像上,分叶、清楚毛糙的界面和胸膜凹陷征对肺部局灶性磨玻璃密度结节的鉴别诊断有一定价值^[7],但对早期肺癌的鉴别有一定局限性。在常规HRCT影像上,AAH通常呈直径6.5 mm以下、圆形或类圆形、边缘光滑、无实性成分、无毛刺、无胸膜牵拉或血管聚集的局灶性磨玻璃影^[8];AIS一般亦为磨玻璃结节,其密度较AAH稍高,有时表现为部分实性结节,偶为实性结节^[9]。在常规HRCT影像上AAH与AIS的鉴别诊断较为困难,其密度差异是诊断的突破口之一。要提高早期肺癌的诊断能力就要求进一步提高检查技术。Sheshadri等^[10]研究发现,减小FOV能明显提高图像的分辨率。Kakinuma等^[11]研究表明,在结节边缘、混杂密度磨玻璃结节混杂密度边缘、空气支气管征、胸膜牵拉等征象的显示方面1 024超高分辨率CT优于常规CT。本研究在进行1 024超高分辨率CT扫描时采用靶扫描技术,下面将从图像显示清晰度和诊断正确率、诊断信心和处理方案、辐射剂量3个方面进行探讨。

首先,在图像显示清晰度和诊断正确率方面,本研究中1 024超高分辨率CT靶扫描不仅对结节边缘及内部混杂密度的显示较常规CT扫描更为清晰,同时也更有助于分辨结节是否为纯磨玻璃结节。相对清晰的内部混杂密度成像可能与1 024超高分辨率CT靶扫描采用小FOV、大矩阵减小了部分容积效应有关。有研究表明磨玻璃结节早期以内部实性成分增长为主要生长模式,且随着结节内肿瘤细胞的增殖越来越具有实性结节的表现^[12]。早期肺癌内部实变或密度增高是其诊断的关键因素,也是导致不同医师之间诊断不一致的主要原因^[13-14]。而本研究中1 024超高分辨率CT靶扫描在诊断正确率上得到了充分的体现,其可以从良性结节(主要指AAH)中识别出更多原位癌。

其次,在诊断信心和处理方案方面,采用1 024超高分辨率CT靶扫描后,3位阅片医师的诊断信心较采用常规CT明显提高。诊断信心的缺乏往往使医师采取较为保守的处理方式,充分的诊断信心则

有助于给出明确的处理建议,对于有恶性倾向的结果,不论大小都应建议尽早手术;能确诊为良性却短时间内不会消除的结节(如肉芽肿等)则应当明确告知,以减少长期随访对患者造成的心理负担以及过度检查带来的辐射问题。值得注意的是,即使部分结节给出的诊断是一致的,但其影像上表现出的密度不均一性有差异,这提示结节内细胞癌变程度和恶性程度不同。此时结合阅片医师的诊断信心,也会出现两种CT扫描诊断结果相同但采用不同处理方案的情况。例如,在本研究中,我们观察到1个结节通过常规CT和1 024超高分辨率CT靶扫描图像都诊断为AIS,但在1 024超高分辨率CT靶扫描图像上此结节表现出更大的密度异质性,阅片医师则会诊断为恶性度更高且诊断信心更充足,从而提出手术的建议;而常规CT图像上,阅片医师则更倾向于随访,以便与AAH相鉴别。本研究结果显示,67个肺结节经过1 024超高分辨率CT靶扫描后,随访病例比常规CT检查明显减少,手术和无需随访例数增加。

最后,从辐射剂量角度看,由于矩阵增大和FOV减小,1 024超高分辨率CT靶扫描需要提高管电流,从而减少噪声,且检查的容积CT剂量指数($CTDI_{vol}$)有所增高。但在实际检查过程中,由于1 024超高分辨率CT靶扫描范围小,患者实际接受的总辐射剂量DLP(剂量长度乘积)平均为191.3 mGy·cm,低于常规CT(平均为280.3 mGy·cm)。当然,如何降低辐射剂量仍是一个需要长期探讨的课题,改进扫描方案、优化重建算法仍值得深入研究。

图像质量的提高和可接受的辐射剂量充分体现了1 024超高分辨率CT靶扫描技术的应用价值。但由于靶扫描的扫描范围有限,无法显示全部肺野,使其应用具有一定的局限性。本研究目的并不是探索靶扫描技术是否可以完全取代常规CT检查,而主要是针对需要高度关注的肺结节,在随访过程中建议采用1 024超高分辨率CT靶扫描代替某次或某一阶段的随访检查,为需高度关注的小结节提供更准确的诊断。

总之,1 024超高分辨率CT靶扫描可以更清晰地显示直径8 mm以下肺结节内部特征尤其是混杂密度成分。对通过常规CT检查难以确诊或诊断信

心不足的结节,建议采用1 024超高分辨率CT靶扫描进一步检查。

[参考文献]

- [1] VERONESI G, MAISONNEUVE P, SPAGGIARI L, RAMPINELLI C, PARDOLESI A, BERTOLOTTI R, et al. Diagnostic performance of low-dose computed tomography screening for lung cancer over five years [J]. *J Thorac Oncol*, 2014, 9: 935-939.
- [2] MAO H, LABH K, HAN F, JIANG S, YANG Y, SUN X. Diagnosis of the invasiveness of lung adenocarcinoma manifesting as ground glass opacities on high-resolution computed tomography [J]. *Thorac Cancer*, 2016, 7: 129-135.
- [3] ABERLE D R, DEMELLO S, BERG C D, BLACK W C, BREWER B, CHURCH T R, et al. Results of the two incidence screenings in the National Lung Screening Trial [J]. *N Engl J Med*, 2013, 369: 920-931.
- [4] National Lung Screening Trial Research Team; ABERLE D R, BERG C D, BLACK W C, CHURCH T R, FAGERSTROM R M, GALEN B, et al. The National Lung Screening Trial: overview and study design [J]. *Radiology*, 2011, 258: 243-253.
- [5] 李惠民,肖湘生,刘士远,李成洲.螺旋CT靶扫描对肺部小结节的诊断价值 [J]. *临床放射学杂志*, 2001, 20: 424-427.
- [6] 毛海霞,韩硠石,项文静,邢彦粉,孙希文.肺腺癌局灶性磨玻璃影的诊断与处理 [J]. *中华结核和呼吸杂志*, 2015, 38: 535-537.
- [7] 范丽,刘士远,李清楚,于红,肖湘生.肺部局灶性磨玻璃密度结节多排螺旋CT征象良恶性的 Logistic 回归分析 [J]. *第二军医大学学报*, 2010, 31: 1060-1064.
FAN L, LIU S Y, LI Q C, YU H, XIAO X S. Multi-detector CT features of benign and malignant pulmonary focal ground-glass opacity nodules: a binary logistic regression analysis [J]. *Acad J Sec Mil Med Univ*, 2010, 31: 1060-1064.
- [8] XIANG W, XING Y, JIANG S, CHEN G, MAO H, LABH K, et al. Morphological factors differentiating between early lung adenocarcinomas appearing as pure ground-glass nodules measuring ≤ 10 mm on thin-section computed tomography [J]. *Cancer Imaging*, 2014, 14: 33.
- [9] AUSTIN J H, GARG K, ABERLE D, YANKELEVITZ D, KURIYAMA K, LEE H J, et al. Radiologic implications of the 2011 classification of adenocarcinoma of the lung [J]. *Radiology*, 2013, 266: 62-71.
- [10] SHESHADRI A, RODRIGUEZ A, CHEN R, KOZLOWSKI J, BURGDORF D, KOCH T, et al. Effect of reducing field of view on multidetector quantitative computed tomography parameters of airway wall thickness in asthma [J]. *J Comput Assist Tomogr*, 2015, 39: 584-590.
- [11] KAKINUMA R, MORIYAMA N, MURAMATSU Y, GOMI S, SUZUKI M, NAGASAWA H, et al. Ultra-high-resolution computed tomography of the lung: image quality of a prototype scanner [J/OL]. *PLoS One*, 2015, 10: e0137165. doi: 10.1371/journal.pone.0137165.
- [12] ZHANG L, YANKELEVITZ D F, CARTER D, HENSCHKE C I, YIP R, REEVES A P. Internal growth of nonsolid lung nodules: radiologic-pathologic correlation [J]. *Radiology*, 2012, 263: 279-286.
- [13] RIDGE C A, YILDIRIM A, BOISELLE P M, FRANQUET T, SCHAEFER-PROKOP C M, TACK D, et al. Differentiating between subsolid and solid pulmonary nodules at CT: inter- and intraobserver agreement between experienced thoracic radiologists [J]. *Radiology*, 2016, 278: 888-896.
- [14] VAN RIEL S J, SÁNCHEZ C I, BANKIER A A, NAIDICH D P, VERSCHAKELEN J, SCHOLTEN E T, et al. Observer variability for classification of pulmonary nodules on low-dose CT images and its effect on nodule management [J]. *Radiology*, 2015, 277: 863-871.

[本文编辑] 杨亚红